ZIBELINE INTERNATIONAL™ PUBLISHING

ISSN: 2521-0920 (Print)
ISSN: 2521-0602 (Online)
CODEN: MJGAAN

Malaysian Journal of Geosciences (MJG)

DOI: http://doi.org/10.26480/mjg.02.2026.80.88

RESEARCH ARTICLE

MINERALOGICAL AND GEOCHEMICAL INSIGHTS INTO LOKOJA SANDSTONES: IMPLICATIONS FOR CLASSIFICATION AND PALEOCLIMATIC RECONSTRUCTION

George U. Ozulu, Michael N. Mba-Otike*,Nkem I. Odiaka, and Chiazor S. Ngozi-Chika

Department of Geology, Dennis Osadebay University, P.M.B. 95090 Asaba, Nigeria
****Corresponding Author Email: mba-otike.michael@dou.edu.ng***

ARTICLE DETAILS

Article History:

Received 26 January 2026
Revised 20 February 2026
Accepted 25 February 2026
Available online 16 March 2026

ABSTRACT

The distribution pattern of major elements' mineralogy and geochemistry in the sandstones of the Lokoja Formation in the Southern Bida Basin of Nigeria was determined and used to classify and decipher the paleoclimatic conditions of the basin. X-ray diffraction (XRD) and X-ray fluorescence (XRF) were utilized to perform mineralogical and inorganic geochemistry investigations on seven (7) typical sandstone samples. Results of the mineralogical analysis, which showed clay matrix and feldspar content in high proportions, helped in interpreting the sandstone as texturally immature, belonging to the wacke clan and classified as feldspathic greywacke. Results of major element concentrations revealed that the sandstone has a depletion of MnO_2 and P_2O_5 and an enrichment of SiO_2, Al_2O_3, Fe_2O_3, CaO, MgO, and Na_2O. Geochemical classification plots, using log ratios of Na_2O/K_2O against SiO_2/Al_2O_3 and SiO_2/Al_2O_3 against K_2O/Na_2O, also show that the sandstone is a greywacke. Similarly, the sandstone was categorised as sodic sandstones rich in plagioclase feldspars using a geochemical ternary diagram of potassium oxide (K_2O) and sodium oxide (Na_2O) overlaid with iron oxide (Fe_2O_3) and magnesia (MgO). The bivariate plot for chemical maturity indicated that the high concentration of feldspars in the photomicrographs indicates a dry paleoclimatic state.

KEYWORDS

Petrography, Mineralogy, Geochemistry, Sandstones, Classification, Paleoclimate, Lokoja Formation

1. INTRODUCTION

The majority of studies on the sedimentary fills in central Nigeria's Southern Bida Basin have focused on elements such as basin geometry, hydrocarbon potentials, stratigraphy/biostratigraphy, sedimentology, and facies analysis (Obaje et al., 2013). Only a few authors like, as well as have given attention to aspects like the petrology, petrography, and geochemistry of the sediments (Madukwe et al., 2014; Sanni et al., 2016; Nton and Adamolekun, 2016). Also interpreted the tectonic settings and origin of the Lokoja Sandstones using petrography and the geochemistry of major and trace elements, building on earlier provenance frameworks established by (Dickinson et al., 2006; Madukwe et al., 2014). To ascertain the tectonic settings, provenance, and pattern of elemental distribution, they also assessed the geochemistry of the main and trace elements, employing methodologies aligned with global standards for sedimentary basin analysis (McLennan et al., 1993 and Priya et al., 2021). They concluded that the majority of the sandstones were mature lithic arenites, protoquartzites, and sub-greywackes from semi-arid to dry climates, consistent with passive margin sedimentation observed in other West African cratonic basins (Rahaman et al., 2019).

While Sanni et al. (2016) used petrographic analysis to demonstrate that the sandstones from the Lokoja Formation are primarily composed of quartz and feldspar mineral, a mineralogical signature typical of felsic source rocks. As combined sedimentological and geochemical data from the Lokoja and Patti Formations to infer the provenance, palaeo-depositional characteristics, and tectonic history of the sediments (Nton and Adamolekun (2016). Their work highlighted the role of weathering indices (e.g., CIA values) in distinguishing between arid and humid paleoclimates (Nesbitt and Young, 1982 and Nikunj et al., 2023). This paper therefore emphasizes the use of mineralogy and geochemistry to determine the elemental distribution pattern, classify, and interpret the paleoclimatic conditions of the sandstones from the Lokoja Formation, bridging a critical gap in the basin's sedimentological narrative.

1.1 Geology of the Study Area

From Shegwa in Niger State to Dekina in Kogi State, the Bida Basin exists as an interior basin with a NW-SE trend, characteristic of Cretaceous rift basins across West Africa (Guiraud et al., 2010; Rahaman et al., 2019). This structural orientation reflects the Pan-African tectonic framework that shaped much of Nigeria's basement complex (Ominigbo, 2022). The basin is strategically located between the West African Craton and the Precambrian Northern Nigeria Massif (Braide, 1992b), a position that influenced its sedimentological evolution during the Late Cretaceous (Obaje, 2009).

In terms of sedimentary fill, this basin forms part of a network of Cretaceous-Tertiary depocenters, joining the Anambra and Sokoto basins in the southeast and northwest extremities, respectively (Ladipo, 1988; Ojo, 2009; Obaje et al., 2011). This tripartite basin system developed during the Santonian tectonic event (~84 Ma) that fragmented the larger Benue Trough (Maravic et al., 1989). According to Ojo and Ajakaiye (1989), the basin's extent is estimated to be over 7,000 km^2, extending from the Niger-Benue Rivers confluence in northwest Nigeria to a maximum width of 160 km in the central Niger region. These dimensions are comparable to other intracratonic sag basins in Africa, such as the Iullemmeden Basin.

Quick Response Code	Access this article online	
	Website: www.myjgeosc.com	**DOI:** 10.26480/mjg.02.2026.80.88

Cite the Article: George U. Ozulu, Michael N. Mba-Otike,Nkem I. Odiaka, and Chiazor S. Ngozi-Chika (2026). Mineralogical and Geochemical Insights into Lokoja Sandstones: Implications for Classification and Paleoclimatic Reconstruction. Malaysian Journal of Geosciences, 10(2): 72-80.

Further constrained the basin's geometry, reporting a breadth ranging from 75 to 150 km and a longest axis of approximately 350 km (Figure 1) (Zaborski, 1998). Gravity measurements by Ojo (1984) revealed a maximum sedimentary succession thickness of approximately 3.5 km along the central axis, consistent with values reported for other failed rift systems (Fosso Téguia et al., 2024). However, proposed an alternative model, suggesting the basin represents a gently down-warped trough within the West and Central African Rift System that maintains a tight genetic relationship to the Benue Trough (Obaje et al., 2011). This interpretation aligns with recent seismic refraction studies showing crustal thinning beneath the basin.

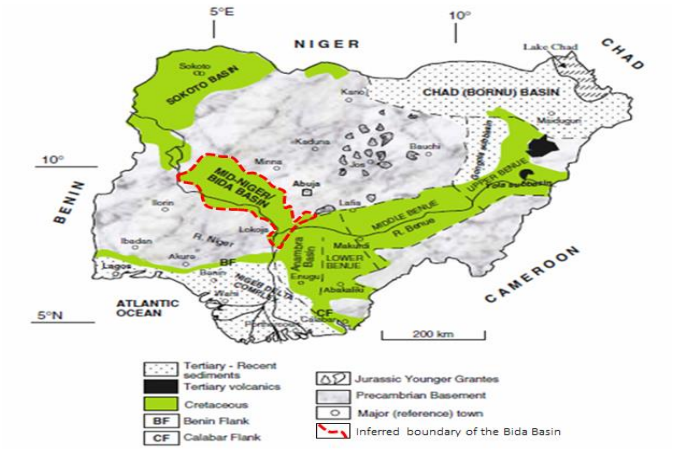

Figure 1: The Bida Basin's location on the Nigerian Geological Map (Obaje et al., 2004).

The Benue Trough's Santonian orogenic motions (~84 Ma) in southeast Nigeria appear to have a close connection with the tectonics that created the Bida Basin, reflecting the regional response to the African-Eurasian plate convergence during the Late Cretaceous (Guiraud 2010). Although they agreed with the cratonic sag model notion, stated that a rift origin might not be completely ruled out, particularly given the basin's NW-SE structural grain that parallels the West African Rift System (Wright et al., 1985; Ojo and Ajakaiye, 1989). Nonetheless, it is widely believed that the basin was formerly a simple intracratonic sag basin, similar to other Cretaceous sag basins like the Illummeden Basin in Niger (Okoro, 2007).

The basic intracratonic sag model appears more likely given the lack of obvious evidence of rift-associated events such as volcanism, igneous intrusions, significant faulting, and sporadic uplifts in the basin. This interpretation is supported by: The absence of syn-rift volcaniclastics in the stratigraphic column (Obaje et al., 2011). Gravity data showing gradual crustal thinning rather than abrupt fault-bounded subsidence (Ojo, 1984), and Low geothermal gradients (<25°C/km) typical of passive sag basins (Nwachukwu, 1976).

The sag model further explains the basin's symmetrical geometry and lack of border faults, contrasting sharply with the adjacent Benue Trough which shows clear rift characteristics. However, some researchers suggest the basin may represent a "failed arm" of the Benue triple junction, explaining its transitional features.

The sedimentary rocks of the southern Bida Basin have been extensively studied, with significant contributions from, (Akande et al., 2005, 2006; Obaje et al., 2011; Omali et al., 2011; Osokpor and Okiti, 2013; Osokpor et al., 2013; Nton and Adamolekan, 2016). These studies collectively reveal a Cretaceous sedimentary succession deposited during a period of major marine transgression-regression cycles across West Africa (Petters, 1986). Originally these sedimentary rocks were divided into three stratigraphic units: the Lokoja Formation, Patti Formation, and Agbaja Ironstone Formation, representing fluvial-deltaic to shallow marine depositional environments comparable to other Upper Cretaceous sequences in the Benue Trough (Ojo and Akande, 2006).

Recent stratigraphic revisions have redefined the nomenclature, with the Patti Formation now formally designated as the Ahoko Formation by (Rahaman et al., 2019; Ozulu et al., 2021). This revision aligns with modern sequence stratigraphic principles and reflects improved biostratigraphic dating of the basin fill (Rahaman *et al.*, 2019).

The Lokoja Formation's lithologic assemblage is particularly diagnostic, comprising: Basal conglomerates (matrix-supported, clast sizes up to 15 cm) marking the initial transgressive phase, Pebbly to coarse-grained sandstones showing trough cross-bedding indicative of fluvial channels, Claystones and siltstones representing floodplain deposits, Ironstone horizons (10-30 cm thick) lateritized during Paleogene weathering and Lateritic capping (2-5 m thick) marking the Cenozoic unconformity (Braide, 1992a; Omali et al., 2011).

This vertical succession records a complete cycle from initial basin subsidence (conglomerates) through fluvial-dominated sedimentation (sandstones) to terminal weathering (ironstones/laterites), mirroring depositional patterns observed in other West African intracratonic basins. The coarse-grained nature of the Lokoja Formation suggests proximity to sediment source areas, likely the Nigerian Basement Complex to the southwest (Obaje et al., 2011).

2. Material and Methods

Both field and laboratory studies were employed as investigative techniques. While X-ray diffraction (XRD) and X-ray fluorescence (XRF) were used in the laboratory mineralogical investigation and inorganic geochemistry, preliminary megascopic identification of minerals in rocks was carried out in the field.

For petrographic examination, seven (7) typical sandstone samples were chosen. For the petrographic analysis, the methods outlined and referenced in Reed and Mergner (1945) were used by (Sorby, 1882). In order to identify minerals under plane polarized light (PPL) and cross polarized light (XPL), seven thin slices were produced and examined using petrographic microscopes. The ternary diagram for the mineral-based apexes of quartz (Q), feldspar (F), and rock (RF) was used to classify sandstone after Pettijohn (1975).

The mineral maturity index formula (MMI) and sandstone limiting values were both used to determine the mineralogical maturity of the Lokoja Sandstones (equation 1 and table 1) (Nwajide and Hoque, 1985).

$$MMI = (\text{Proportion of Q})/(\text{Proportion of F} + \text{Proportion of R.F}) \quad (1)$$

Where MMI is the Mineralogical Maturity Index.

Table 1: Recovery rates of MSWI residue samples after separation using a cyclosizer

Limiting % of Q and (F + RF)	Maturity Stage and MI
Q ≥ 95% (F+RF) = 5%	MI ≥ 19 Super-mature
Q = 95-90% (F+RF) = 5 - 10%	MI = 19-9.0 Sub-mature
Q = 90-75% (F+RF) = 10 - 25%	MI = 9.0-3.0 Sub-mature
Q = 75-50% (F+RF) = 25 - 50%	MI = 3.0-1.0 Immature
Q < 50%	MI ≤ 1
(F+RF) > 50%	Extremely Immature

The sandstones' bulk and clay minerals were analyzed using X-Ray Diffraction (XRD). For this investigation, a Philips PANalytical device with a pw 3830 X-ray generator running at 40 kV and 25 mA was employed. To eliminate the adsorbed water, the ground-up samples were oven-dried for 12 hours at 100 °C. Using a spatula cleaned with alcohol, the samples were squeezed into rectangular aluminum sample holders, which were then clipped into the instrument sample holder. After then, the samples were tallied for 0.5 seconds every step from 5 to 85 degrees and scanned on a 2 theta scale at intervals of 0.02 seconds.

Only an intensity plot as a function of 2θ was produced by the XRD machine, but the diffraction patterns it recorded were similar to the "fingerprint" of crystalline materials and could be compared to conventional patterns to identify new materials. The x-ray diffractogram displaying the spectrum signatures of the minerals present reflects the analysis's findings.

Seven (7) sandstone samples were subjected to X-ray fluorescence (XRF) in order to identify the main components present. Using a 2.4 kW Rh X-ray tube, the Philips Empyrean PANalytical Machine was used to grind up and analyze the sandstone samples. 1.00 g of the sample was weighed and dried for an hour at 110oC as part of the analytical procedures for major element analysis. After that, 10.00 g of Claisse flux was added, and it was fused for 23 minutes in the Claisse fluxer. The mixture was then supplemented with 0.2 g of Na2CO3. The sample, flux, and Na2CO3 have now been pre-oxidized at 700 °C prior to fusion. Ultrapure Fused Anhydrous Li-Tetraborate-Li-Metaborate (66.67% Li2B4O7 + 32.83%

LiBO2) was the type of flux utilized, while Li-iodide (0.5%) was used as a releasing agent. The method uses percentage (%) oxides to report the concentration of key elements. Ten (10) key elements were determined to have oxide percentages using this analytical method: silicon (Si), aluminum (Al), iron (Fe), calcium (Ca), magnesium (Mg), potassium (K), sodium (Na), titanium (Ti), manganese (Mn), and phosphorus (P).

In a test known as loss on ignition (LOI), samples of the material under study are heated to a high enough temperature to cause volatile compounds to escape. Until its mass stops changing, oxygen is added. To ascertain their inherent moisture contents, the produced samples were oven-dried for an entire night at a predetermined temperature (1050C). After that, the samples were once more baked for an entire night at a different temperature (800 0C), and the weight difference was calculated to calculate the loss on ignition (LOI). The volatile compounds of H2O, OH-, CO2, F-, Cl-, and S contribute to the LOI, as do K+ and Na+ (if heated for an extended period of time); or, alternatively, compounds of oxygen (O2) added by oxidation, such as FeO to Fe2O3, and later carbon-dioxide (CO2), such as CaO to CaCO3.

3. Results

From the findings of the petrographic analysis, the predominant minerals are feldspar and quartz, with a few lithic (rock) fragments serving as framework elements. Figures 2-8 display the photomicrographs used for the petrographic study, and Tables 3a and 3b provide the petrographic analysis data and a description of the mineralogical composition of the sandstone samples. Silt/clay size quartz, mica, clay, and iron oxide are the minerals that fill the voids. Silt-sized quartz and uncrystallised clay make up the matrix, and iron oxide serves as the binding agent. Under cross-polarized light, the majority of quartz minerals exhibit straight to undulose extinction, while the margins of the majority of individual quartz grains are fractured and have sutures, which is a sign of tectonic activity. Because some plagioclase minerals are untangled, it can be challenging to distinguish them from both quartz and one another.

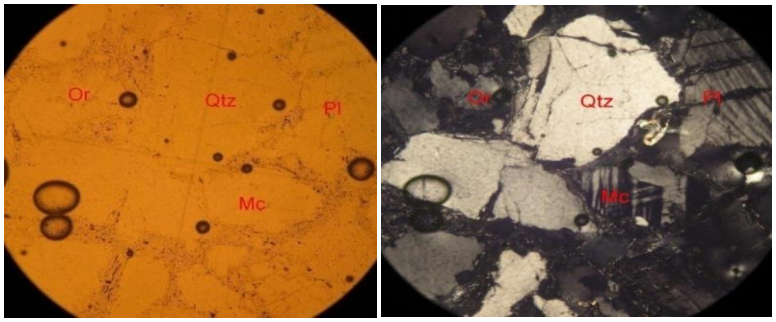

Figure 2: Photomicrograph of LKJ 1 Sandstone Sample: (a) PPL and (b) XPL, displaying microcline, albite, orthoclase feldspar, and subrounded quartz

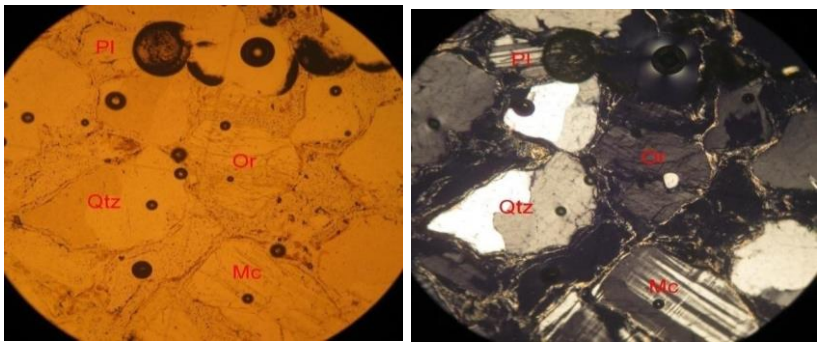

Figure 3: The LKJ 2 Sandstone Sample photomicrographs (a) PPL and (b) XPL display microcline, sub-rounded quartz, orthoclase feldspar, and plagioclase

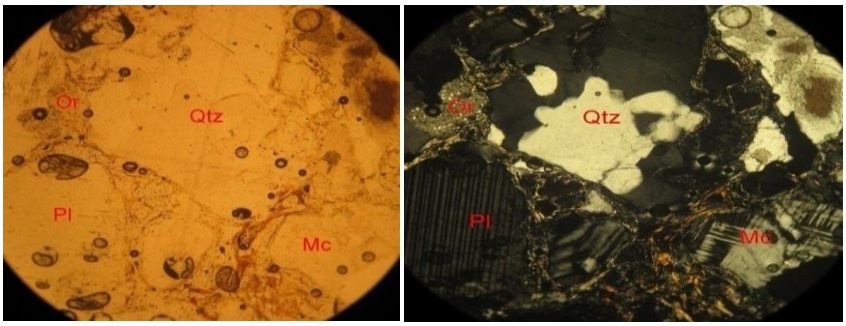

Figure 4: The LKJ 3 Sandstone Sample photomicrographs (a) PPL and (b) XPL display microcline, sub-rounded quartz, orthoclase feldspar, and plagioclase.

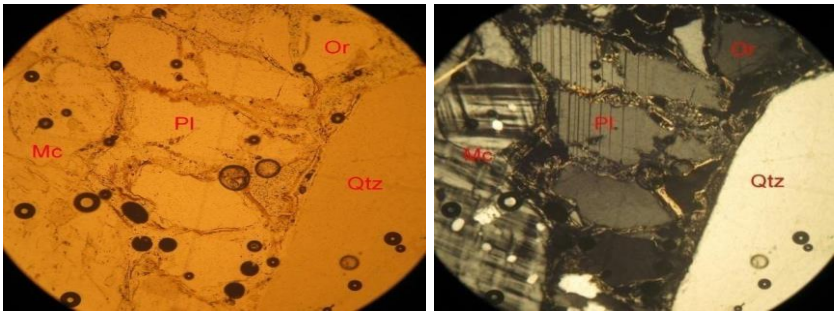

Figure 5: The LKJ 4 Sandstone Sample photomicrographs (a) PPL and (b) XPL display microcline, sub-rounded quartz, orthoclase feldspar, and plagioclase

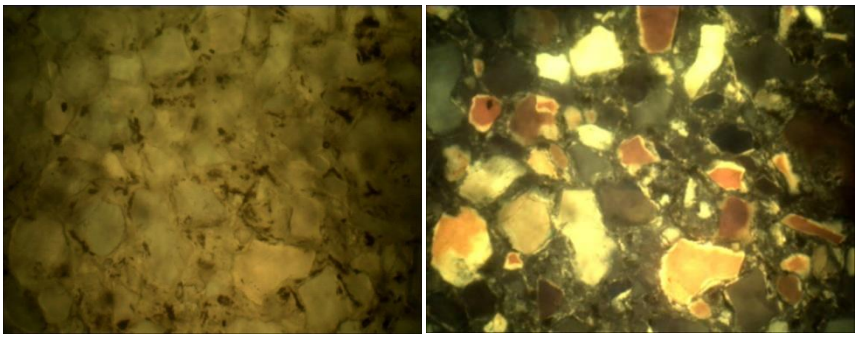

Figure 6: Photomicrograph of LKJ 5 Sandstone Sample: (a) PPL and (b) XPL displaying microcline, albite, orthoclase feldspar, and sub-rounded quartz

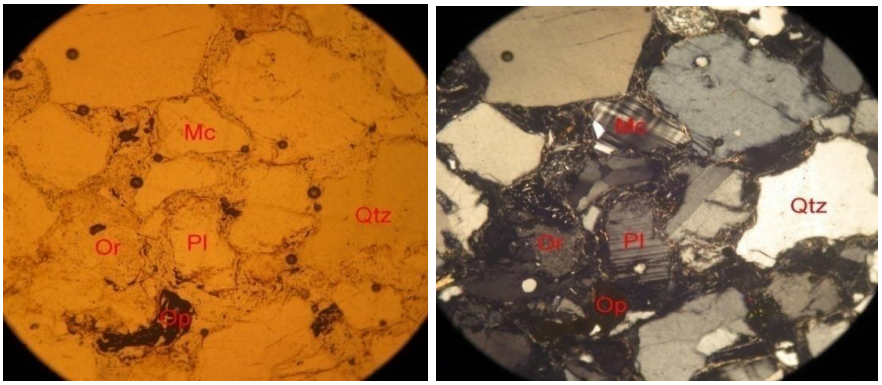

Figure 7: LKJ 6 Sandstone Sample Photomicrograph: (a) PPL and (b) XPL displaying sub-rounded quartz and feldspar

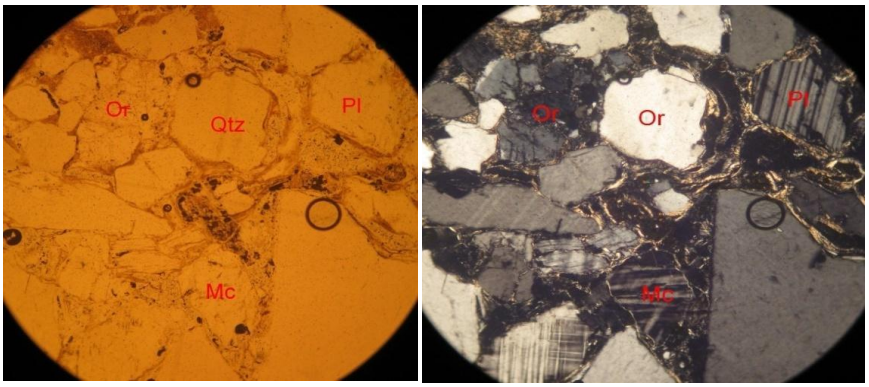

Figure 8: LKJ 7 Sandstone Sample Photomicrograph: (a) PPL and (b) XPL displaying sub-rounded quartz and feldspar.

Key: Mtx stands for matrix, Mc for microcline, Alb for albite, Pl for plagioclase, Or for orthoclase, and Qtz for quartz.

The modal content of the sandstones and the composition of the detrital framework are displayed in Tables 2 and 3, respectively. Rock fragments range from 3.13 to 4.42% with an average of 3.72%, matrix and cement from 15.32 to 20.33% with an average of 17.96%, unfilled voids from 2.10 to 4.43% with an average of 3.47%, and quartz from 36.81 to 46.67% with an average of 42.42%. About 90% of all quartz is monocrystalline, with the remaining 10% being polycrystalline.

Table 2: Data from petrographic analysis displaying the overall sandstone composition in the research area (%)

Sample No.	Quartz %	Feldspar %	Rock Fragments %	Matrix and Cement %	Unfilled Void %
LKJ1	41.76	37.36	3.46	15.32	2.10
LKJ2	36.81	35.71	4.42	18.63	4.43
LKJ3	37.77	35.00	4.07	19.64	3.56
LKJ4	41.67	29.76	4.08	20.33	4.16
LKJ5	46.67	29.70	3.45	17.13	3.05
LKJ6	46.42	28.58	3.42	18.24	3.34
LKJ7	45.84	30.95	3.13	16.42	3.66
Average Value	42.42	32.44	3.72	17.96	3.47

Key: Felele (LKJ1), Felele (LKJ2), Nataco (LKJ3), Nataco (LKJ4), Oworo Estate (LKJ5), Banda (LKJ6), and Banda (LKJ7)

Table 3: Summary of Sandstone Samples' Mineralogical Composition (%) Using the Recalculated Sandstone Sample Framework for the Study Area.

Sample Nos.	Quartz	Feldspar	Rock Fragments	MMI
LKJ1	50.57	45.24	4.17	1.02
LKJ2	47.84	46.41	5.74	0.92
LKJ3	49.15	45.55	5.30	0.97
LKJ4	55.18	39.41	5.40	1.23
LKJ5	58.47	37.21	4.32	1.41
LKJ6	59.19	36.44	4.36	1.45
LKJ7	57.36	38.73	3.92	1.34
AverageValue	53.98	41.28	4.73	1.17

There are two ways to interpret the composition of the Lokoja Sandstones: mineralogical maturity and textural maturity. As textural maturity flow charts served as the foundation for the evaluation of textural maturity (Pettijohn's, 1975). The average matrix (clay) and cement percentage of the sandstones is 17.96%, or 15%, according to Table 2. Thus, because to inadequate sorting and a clay component of more than 15%, the Lokoja Sandstone is considered texturally immature. The significance of matrix in separating sandstones into the arenite and wacke clans is acknowledged both categorization scheme (Pettijohn's, 1975; Bogg's, 2006). The Wacke clan is represented by sandstones with 15% or more matrices, and the Arenite clan is represented by those with less than 15%. A textural element called the matrix influences the sandstone's porosity and indicates how fluid the transporting medium is (Pettijohn, 1975). The Lokoja Sandstones' average matrix composition of more than 15% indicates that they are Wacke clan members. The sandstones are classified as feldspathic (arkosic) wacke by the recalculated framework composition, which shows an average feldspar of 41.28% (table 3) (Figure 9).

The Lokoja Sandstone has been classified as either feldspathic or arkosic by certain scientists using the classification scheme, which totally ignores the matrix as a crucial component in sandstone classification (Folk, 1974).

The mineralogical maturity index (MMI) developed was used to determine the mineralogical maturity by (Nwajide and Hoque, 1985). The Lokoja Sandstone has an average mineralogical maturity index (MMI) of 1.17, with values ranging from 0.92 to 1.45 (table 1). It is believed that the sandstones are mineralogically immature because the MMI value is > 3.0 but > 1.0. According to table 1, the Lokoja sandstone typically contains 42.42 percent quartz, 32.44 percent feldspar, 3.72% rock fragments, 17.96% matrix and cement fraction, and 3.47% empty voids. As defined MI as super-mature if it is greater than 19, mature if it is between 19 and 9, sub-mature if it is between 9 and 3, immature if it is between 3 and 1, and severely immature if it is less than 1 (Nwajide and Hoque, 1985).

MMI = Mineralogical Maturity Index

Mineralogical maturity index (MMI) is given as Qtz/(Fsp + Lf), that is (total quartz)/(feldspar + lithic fragments).

Average MMI = Quartz (Q) = 53.98, Feldspar (F) = 41.28, Rock Fragments (RF) = 4.73 (see table 3).

MMI = 53.98/41.28 + 4.73 = 1.1

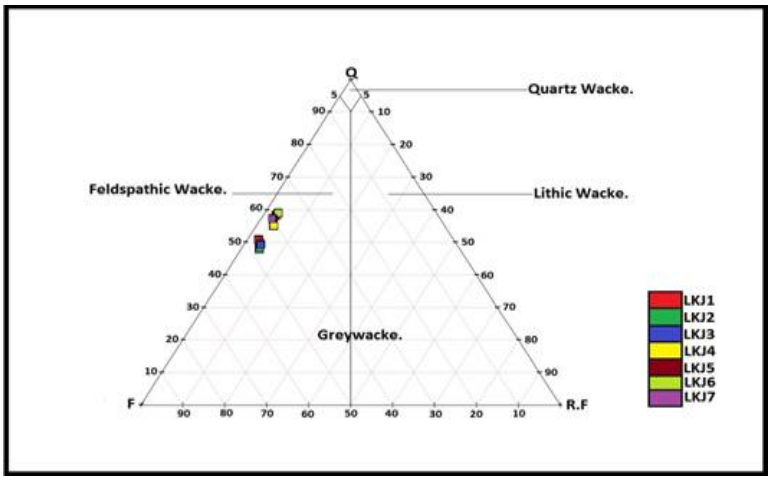

Figure 9: Sandstone-mineral base classification in the study area using the QFRF Ternary Diagram (following Pettijohn, 1975)

The mineral assemblage is dominated by quartz and feldspar, according to X-ray diffraction (XRD) studies, indicating a mild weathering profile for the Lokoja Sandstones. Orthoclase, microcline, and albite are among the feldspars; muscovite, kaolinite, enstatite, and rutile are further related minerals (see Figure 10).

Table 4 reports the principal element concentrations of the sandstones in the study region as oxide percent by weight. Iron (Fe), calcium (Ca), magnesium (Mg), potassium (K), sodium (Na), titanium (Ti), manganese (Mn), silicon (Si), iron (Al), and phosphorus (P) are among them. X-ray fluorescence (XRF) was used to identify the elemental compositions of the samples, and the sandstones were classified based on the concentration of the three main oxide groups: silica, alumina, and alkali oxides, along with iron oxides and magnesia. According to the findings, the sandstone is low in MnO_2 and P_2O_5 and enriched in SiO_2, Al_2O_3, Fe_2O_3, CaO, MgO, and Na_2O. The average value (0.91) of the potassium oxide (K_2O) content (0.82-0.98) is < unity (1), suggesting a somewhat lower concentration of K-feldspar than plagioclase feldspar. Ca-rich and Na-rich plagioclase feldspars that may have originated from basic and felsic igneous or metamorphic rocks are indicated by the enrichment of CaO and Na_2O unity (1) in all samples. The low concentration of the oxide in the source region may be the cause of the low value of K_2O in comparison to CaO and Na_2O. Compared to the orthoclase feldspar, the plagioclase is observed to be more prevalent in the thin sections. The significant amounts of quartz and kaolinite as components mostly reflect the high levels of silica (SiO_2) and alumina (Al_2O_3). The source rocks may contain a lot of felsic minerals, as shown by the somewhat elevated titanium oxide (TiO_2) percentage (1.10-2.41%). Since titanium is more stationary than other elements during different sedimentary processes, its high concentration in sandstone indicates that the progenitor (source) rock is abundant (Nton and Adamolekun, 2016). The presence of the heavy minerals may be the cause of the high iron (Fe_2O_3) concentration, whereas biotite, a ferromagnesian mineral, may be the source of magnesium oxide (MgO).

Table 4: Major elemental oxide content of the research area's sandstones (%)

Sample	SiO_2	Fe_2O_3	MgO	CaO	Al_2O_3	K_2O	Na_2O	TiO_2	MnO_2	P_2O_5	LOI
Lokoja1	57.50	7.90	1.55	4.70	24.60	0.88	1.25	1.10	0.04	0.28	0.41
Lokoja2	57.46	7.89	1.50	4.67	23.78	0.98	1.30	1.12	0.05	0.27	1.08
Lokoja3	57.60	8.78	1.78	3.86	23.68	0.97	1.32	1.44	0.02	0.35	0.69
Lokoja4	56.78	8.67	1.77	3.88	23.77	0.98	1.30	1.45	0.03	0.33	1.55
Lokoja5	57.67	7.89	1.56	4.67	24.56	0.89	1.26	1.12	0.05	0.26	0.57
Lokoja6	59.36	6.63	2.47	4.27	22.06	0.82	1.52	2.40	0.02	0.43	0.22
Lokoja7	58.98	6.46	2.40	4.24	22.12	0.88	1.56	2.41	0.03	0.43	0.85
Min	56.78	6.63	1.50	3.86	22.06	0.82	1.25	1.10	0.02	0.26	0.22
Max	59.36	8.78	2.47	4.70	24.60	0.98	1.56	2.41	0.05	0.43	1.55
Av.	57.91	7.75	1.86	4.33	23.51	0.91	1.36	1.58	0.03	0.34	0.77

According to numerous reports, clastic sediments' geochemical signatures can be used to infer information about their provenance (Taylor and Mclennan, 1985; Cullers, 1995; Armstrong-Altrin et al. 2004; Okunlola and Idowu, 2012). The relationships between the major elements—SiO_2/Al_2O_3 (2.47), Na_2O/K_2O (1.51), K_2O/Na_2O (0.71), and Fe_2O_3+MgO (9.79) are displayed by the average major elemental oxides ratios (see table 4). The sandstones' Al_2O_3/Ti_2O ratio range (9.19-22.36) points to intermediate to felsic source rocks. The Al_2O_3/Ti_2O ratio rises from 3 to 8 for mafic igneous rocks, 8 to 21 for intermediate rocks, and 21 to 70 for felsic igneous rocks, according to (Hayashi et al., 1997). While the high value of Fe_2O_3+MgO indicates contribution from ferromagnesian minerals from a mafic source provenance, the comparative values of the sodium/potassium alkali ratio (Na_2O/K_2O) (1.51) and the potassium/sodium alkali ratio (K_2O/Na_2O) (0.71) demonstrate the dominance of Na-rich feldspar to the k-feldspar.

Several geochemical diagrams have been used to show the chemical classification of the Lokoja Sandstones, their provenance and tectonic setting. These include those of (Pettijohn, et al., 1972; Lindsey, 1999; Al-Juboury, 2007). The geochemical classification of the Lokoja Sandstones was investigated using the log ratios of Na_2O/K_2O plotted against the log ratios of SiO_2/Al_2O_3 and the log ratios of SiO_2/Al_2O_3 plotted against the log ratios of K_2O/Na_2O (figures 10 and 11) (Pettijohn et al., 1972; Lindsey, 1999).

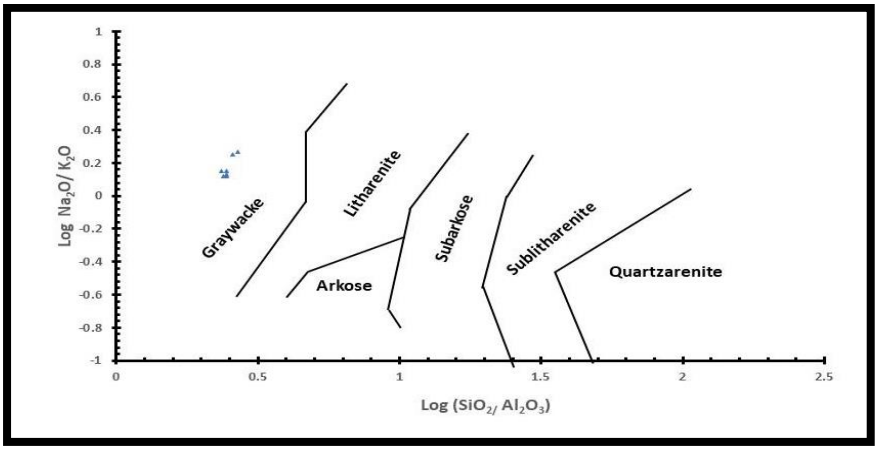

Figure 10: Log ratios of SiO_2/Al_2O_3 versus Na_2O/K_2O were used to classify the Lokoja Sandstones chemically by (Pettijohn et al., 1972).

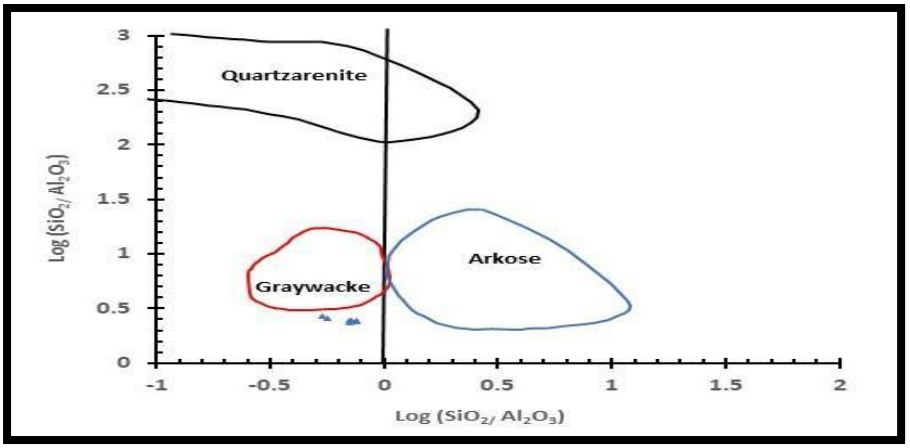

Figure 11: Major classifications of sandstones' compositional fields using log ratios of SiO_2/Al_2O_3 vs. log ratios of K_2O/Na_2O (Lindsey, 1999)

The most often used geochemical parameters for distinguishing between mature and immature sediments are the SiO2 concentration and the SiO2/Al2O3 ratio, which also indicate the abundance of quartz, feldspar, and clay components (Potter, 1978). The figure had the Lokoja Sandstones displayed as greywacke (Pettijohn et al., 1972). By substituting the log ratio of SiO2/Al2O3 along the Y-axis for log Na2O/K2O, Lindsey (1999) adjusted the diagram and depicted the sandstones in the greywacke zone evenly (Pettijohn et al., 1972). The most unusual feature of the

geochemical classification of the sandstones is that they are all dispersed throughout the Greywacke region and have similar compositions. According to the story, greywackes are juvenile sandstones with a matrix value of 15% of the overall sandstone composition (Potter, 1978). As a result, the sandstones were classified as greywacke thanks to the 15% matrix content. Due to the high feldspar content, the sandstone was first classified as feldspathic greywacke using Pettijohn's (1975) QFL Ternary diagram (Figure 9). Relatively juvenile sand deposits are indicated by the high feldspar concentration (potassic and plagioclase) (Malick and Ishiga, 2016).

The sandstone was also categorized as greywacke using Lindsey's (1999) classification guide. Table 4 shows that the average value of log SiO2/Al2O3 is 0.39, which is less than 1, and log K2O/Na2O is -0.17, which is less than 0. Lindsey's (1999) classification guideline states: For quartz arenites, log (SiO2/Al2O3) ≥ 1.5; for greywackes, log (SiO2/Al2O3) < 1 and log (K2O/Na2O) < 0. For arkoses (including sub-arkose), log (SiO2/Al2O3) < 1.5 and log (K2O/Na2O) ≥ 0 and log (Fe2O3+MgO)/(K2O+Na2O) < 0 is required; for lithic arenites (sub-greywacke, including protoquartzite), log (SiO2/Al2O3) < 1.5 and either log (K2O/Na2O) < 0 or log (Fe2O3+MgO)/(K2O+Na2O) ≥ 0 if log (K2O/Na2O) < 0. To confirm the type of sandstone, a further classification was carried out using Blatt et al. (1972)'s ternary diagram. The sandstone was classified as sodic sandstones rich in plagioclase feldspars using potassium oxide (K2O), sodium oxide (Na2O), iron oxide (Fe2O3), and magnesia (MgO) (Figure 12). The computed ratios of sandstone oxides and logs for chemical classification as well as the recalculated oxides for the chemical classification of the Lokoja Sandstone have been shown in tables 5 and 6.

Table 5: Determined the sandstone oxide and log ratios for the research area's chemical categorization

Sample	SiO_2/Al_2O_3	TiO_2/Al_2O_3	Al_2O_3/TiO_2	K_2O/Na_2O	Na_2O/K_2O	Fe_2O_3/K_2O	$Fe_2O_3 + MgO$	$Na_2O + K2O$	$(Fe_2O_3 + MgO)/Na_2O + K_2O$	$(Fe_2O_3 + MgO)/Na_2O$	Log (SiO_2/Al_2O_3)	Log (K_2O/Na_2O)	Log $(Fe_2O_3 + MgO)/Na_2O + K_2O$	Log $(Fe_2O_3 + MgO)/Na_2O$
LKJ1	2.34	0.05	22.36	0.70	1.42	8.98	9.45	2.13	4.44	7.56	0.37	-0.15	0.65	0.88
LKJ2	2.38	0.05	22.56	0.75	1.33	8.05	9.98	2.28	4.38	7.68	0.38	-0.12	0.64	0.89
LKJ3	2.43	0.06	16.44	0.73	1.36	9.05	10.56	2.29	4.61	8.00	0.39	-0.14	0.66	0.90
LKJ4	2.47	0.08	17.98	0.75	1.33	8.85	10.44	2.28	4.58	8.03	0.39	-0.12	0.66	0.90
LKJ5	2.44	0.91	16.56	0.71	1.42	8.87	9.87	2.15	4.59	7.85	0.39	-0.15	0.66	0.89
LKJ6	2.69	0.11	9.19	0.54	1.85	8.09	9.10	2.34	3.89	5.99	0.43	-0.27	0.59	0.78
LKJ7	2.56	0.14	10.01	0.56	1.77	7.34	9.14	2.44	3.75	5.86	0.41	-0.25	0.57	0.77
Min.	2.34	0.05	9.19	0.54	1.33	7.34	9.10	2.13	3.75	5.86	0.37	-0.27	0.57	0.77
Max.	2.69	0.14	22.36	0.75	1.85	9.05	10.56	2.44	4.59	8.03	0.43	-0.12	0.66	0.90
Avg.	2.47	0.20	16.44	0.71	1.50	8.46	9.79	2.27	4.32	7.28	0.39	-0.17	0.63	0.86

Table 6: Recalculated oxides (%) for the Lokoja Sandstone's chemical categorization

Sample No	Fe_2O_3+ MgO (%)	Na_2O (%)	K_2O (%)
LKJ1	81.61	10.79	7.60
LKJ2	81.40	10.61	7.99
LKJ3	82.18	10.27	7.55
LKJ4	82.08	10.22	7.70
LKJ5	82.11	10.48	7.41
LKJ6	79.54	13.29	7.17
LKJ7	78.93	13.47	7.60

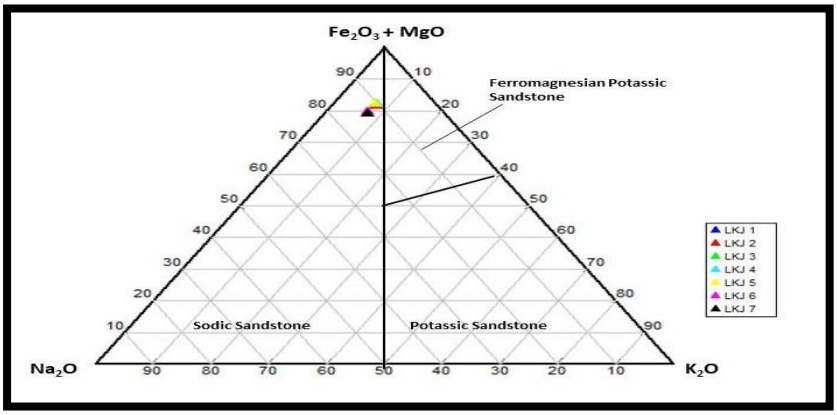

Figure 12: The Lokoja Sandstone's ternary plot (after Blatt et al., 1972)

Figure 13 displays bivariate plot of SiO_2 (quartz content) against Al_2O_3 + K_2O + Na_2O (feldspar content), which depicts the chemical maturity trend as a function of climate (Suttner and Dutta's, 1986). The plotted samples demonstrate the region's arid climate, which is trending toward greater chemical maturity. The samples' immaturity is further demonstrated by the bivariate plot of the quartz-matrix ratio SiO_2/Al_2O_3 against the mineralogical maturity index (MMI) (Figure 14) by (Al-Juboury, 2007).

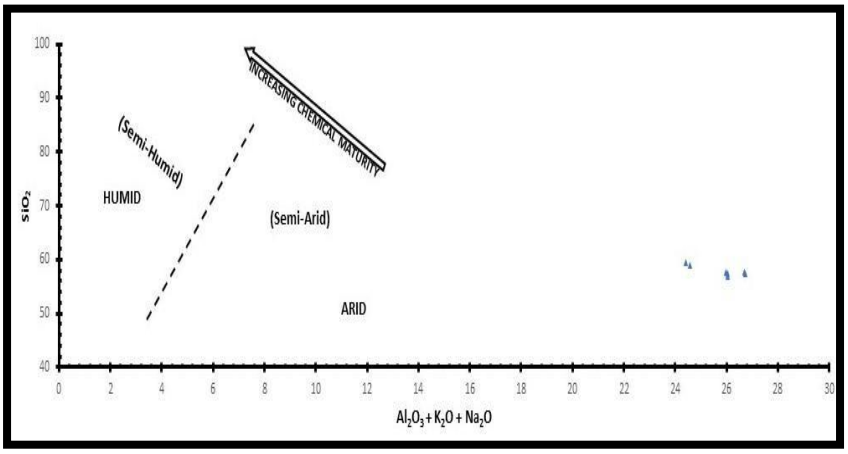

Figure 13: Bivariate figure showing Lokoja Sandstone's chemical maturity (after Suttner and Dutta, 1986)

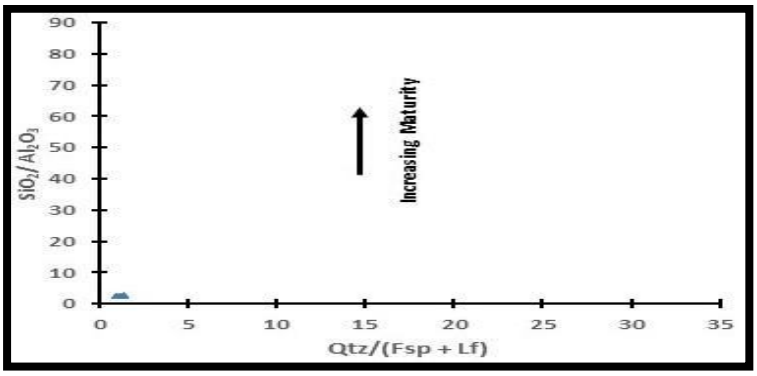

Figure 14: The Lokoja Sandstone's chemical maturity bivariate plot (after Al-Juboury, 2007)

4. Discussion

The detrital feldspars served as important markers of the rocks' paleoclimatic conditions, and both the mineralogical and geochemical investigations offered helpful hints on how to recognize and categorize the rocks as well as interpret their paleoclimatic circumstances.

There are two ways to interpret the composition of the Lokoja Sandstones: mineralogical maturity and textural maturity. While mineralogical maturity was inferred using mineralogical maturity index (MMI), textural maturity was assessed using textural maturity flow chart (Nwajide and Hoque's, 1985; Pettijohn's, 1975). The average matrix and cement content of 17.96%, or > 15%, and the average mineralogical maturity index (MMI) values of 1.17, which are < 3.0 but > 1.0, have been regarded as both texturally and mineralogically immature.

The Lokoja sandstones were classified as arkose to subarkose using the textural maturity flow chart, and as lithic arenites (containing sub-greywacke and protoquartzites) using the scheme (Sanni et al., 2016; Folk, 1974; Blatt et al., 1972). Although had previously noted a greater proportion of cement and sodic plagioclase in the sandstones, they ultimately did not take this into account when classifying the rocks (Bassey and Eminue, 2013).

As ascribed the low SiO_2/Al_2O_3 ratio to the high degree of clay content, which suggests that the sandstones are mineralogically immature (Odundun and Ogundoro, 2019). The Lokoja Sandstones are now classified as greywackes based on their cement concentration of 15% and percentage matrix. The sandstones were further verified as greywackes by plots on the classification diagrams of (Lindsey, 1999; Pettijohn et al., 1972). It is totally inaccurate to classify the Lokoja sandstones using the Folk (1974) classification scheme, which only takes the matrix composition into account by 15%. The ternary diagram further characterized the sandstone as sodic sandstones that are abundant in plagioclase feldspars of (Blatt et al., 1972). While comparative values of sodium/potassium alkali ratio (Na_2O/K_2O) (1.51) and potassium/sodium alkali ratio (K_2O/Na_2O) (0.71) (table 5) indicate the dominance of Na-rich feldspar over k-feldspar, the work's major elements and oxides results strongly suggest intermediate to felsic source rocks (table 4).

The amount of detrital feldspar in sandstones is a crucial indicator of their paleoclimate (Folk, 1974; Igwe et al., 2013). A dry climate is supported by the high percentage of feldspars visible in the photomicrographs. The presence of highly chemically worn and depleted feldspars would indicate a humid climate regardless of the proximity to the depositional basin. The meteorological conditions in the source location were also inferred using the graphic created by Suttner and Dutta (1986). As proposed a bivariate plot of SiO_2 (quartz content) against Al_2O_3 + K_2O + Na_2O (feldspar content) (Figure 14), which shows the trend of chemical maturity as a function of climate (Suttner and Dutta, 1986). The samples were plotted in an arid climate in the region that was trending toward increasing chemical maturity. The bivariate plot of the quartz-matrix ratio SiO_2/Al_2O_3 against the mineralogical maturity index (MMI) (Figure 15) further supports this by (Al-Juboury, 2007).

5. Conclusions

Results from the mineralogical and inorganic geochemical analyses show that the Lokoja sandstones are texturally, mineralogically and chemically immature classified as sodic feldspathic greywackes rich in plagioclase feldspars. The high amount of feldspars, seen in the photomicrographs and confirmed by the bivariate plot for chemical maturity, supports a dry arid to semi-arid paleoclimatic conditions.

References

Akande, S. O., Ojo, O. J., Adekeye, O. A., and Ladipo, K. O., 2006. A geological field guide to the Southern Bida Basin. Nigerian Association of Petroleum Explorationists (NAPE).

Akande, S. O., Ojo, O. J., Erdtmann, B. D., and Hetenyi, M., 2005. Paleoenvironments, organic petrology and Rock-Eval studies on source rock facies of the Lower Maastrichtian Patti Formation, Southern Bida Basin Nigeria. Journal of African Earth Sciences, 8, Pp. 394-406.

Blatt, H., Middleton, G., and Murray, R., 1972. Origin of sedimentary rocks. Prentice-Hall.

Braide, S. P., 1992a. Geological development, origin and energy mineral resources potential of the Lokoja Formation in the Southern Bida

Basin. Journal of Mining and Geology, 28(1), Pp. 33-44.

Braide, S. P., 1992b. Syntectonic fluvial sedimentation in the Central Bida Basin. Journal of Mining and Geology, 28(1), Pp. 55-63.

Dickinson, W. R., 2006. Temper sands in prehistoric Oceanian pottery: Geotectonics, sedimentology, petrography, provenance. Geological Society of America Bulletin, 94, Pp. 222-235.

Folk, R. L., 1974. Petrology of sedimentary rocks. Hemphill.

Fosso Téguia, M. E. E., Ebbing, J., Haas, P., and Szwillus, W., 2024. Integrated geophysical-petrological 3D-modeling of the West and Central African Rift System and its adjoining areas. Journal of Geophysical Research: Solid Earth, 129(7), e2024JB029226.

Guiraud, M., Buta-Neto, A., and Quesne, D., 2010. Segmentation and differential post-rift uplift at the Angola margin as recorded by the transform-rifted Benguela and oblique-to-orthogonal-rifted Kwanza basins. Marine and Petroleum Geology, 27(5), Pp. 1040-1068.

Hayashi, K., Fujisawa, H., Holland, H., and Ohmoto, H., 1997. Geochemistry of 1.9 Ga sedimentary rocks from northeastern Labrador, Canada. Geochimica et Cosmochimica Acta, 61(19), Pp. 4115-4137.

Hoque, M., and Nwajide, C. S., 1985. Application of Markov chain and entropy analysis to lithologic successions: An example from the Cretaceous of the Benue Trough (Nigeria). Geologische Rundschau, 74, Pp. 165-177.

Igwe, E. O., Amoke, G. U., and Ngwu, C. N., 2013. Provenance and tectonic setting of Amasiri Sandstone (Turonian) in Ugep area, Southern Benue Trough, Nigeria: Evidences from petrography and geochemistry. Global Journal of Science Frontier Research: Environment and Earth Science, 13(2), Pp. 32-40.

Madukwe, H. Y., Akinyemi, S. A., Adebayo, O. F., Ojo, A. O., Aturamu, A. O., and Afolagboye, L. O., 2014. Geochemical and petrographic studies of Lokoja Sandstone: Implications on source area weathering, provenance and tectonic setting. International Journal of Scientific and Technology Research, 3(12), Pp. 65-89.

Malick, B. M. L., and Ishiga, H., 2016. Geochemical classification and determination of maturity source weathering in beach sands of Eastern San'in Coast, Tango Peninsula, and Wakasa Bay, Japan. Earth Science Research, 5(1), Pp. 44-56.

Maravic, H. V., Morteani, G., and Roethe, G., 1989. The cancrinite-syenite/carbonatite complex of Lueshe, Kivu/NE-Zaire: Petrographic and geochemical studies and its economic significance. Journal of African Earth Sciences, 9(2), Pp. 341-355.

Nesbitt, H. W., and Young, G. M., 1982. Early Proterozoic climates and plate motions inferred from major element chemistry of lutites. Nature, 299(5885), Pp. 715-717.

Nikunj, K., Shivam, M., Chandrakant, G., and More, L., 2023. Texture and major element geochemistry of channel sediments in the Orsang and Hiren River Basins, Gujarat, India: Implications for provenance and weathering. Journal of the Indian Association of Sedimentologists, 40(2), Pp. 57-67.

Nton, M. E., and Adamolekun, O. J., 2016. Sedimentological and geochemical characteristics of outcrop sediments of Southern Bida Basin, Central Nigeria: Implications for provenance, paleoenvironment and tectonic history. Ife Journal of Science, 18(2), Pp. 345-369.

Nwajide, C. S., and Hoque, M., 1985. Problem of classification and maturity-evaluation of diagnostically altered fluvial sandstone. Geologie en Mijnbouw, 64, Pp. 67-70.

Obaje, N. G., 2009. Geology and mineral resources of Nigeria. Springer.

Obaje, N. G., Moumouni, A., Goki, N. G., and Chaanda, M. S., 2011. Stratigraphy, paleogeography and hydrocarbon resource potentials of the Bida Basin in North-Central Nigeria. Journal of Mining and Geology, 47(2), Pp. 97-113.

Obaje, N. G., Wehner, H., Scheeder, G., Abubakar, M. B., and Jaura, A., 2004. Hydrocarbon prospectivity of Nigeria's inland basins: From the viewpoint of organic geochemistry and organic petrology. AAPG Bulletin, 87, Pp. 325-353.

Ojo, O. J., and Akande, S. O., 2006. Sedimentology and palynological studies of the Patti Formation, Southern Bida Basin, Nigeria: Implications for paleoenvironments and paleogeography. NAPE Bulletin, 19, Pp. 61-77.

Ojo, S. B., 1984. Middle Niger Basin revisited: Magnetic constraints on gravity interpretations. Nigerian Mining and Geosciences Society Conference, Nsukka, Nigeria (Abstract).

Ojo, S. B., and Ajakaiye, D. E., 1989. Preliminary interpretation of gravity measurements in the Mid-Niger Basin area Nigeria. In C. A. Kogbe (Ed.), Geology of Nigeria (2nd ed., pp. 347-358). Rock View (Nigeria) Limited.

Okoro, A. U., 2007. Lithofacies and depositional environments of the Bida Sandstones, Bida Basin Nigeria. Journal of Applied and Natural Sciences, 1(1), Pp. 64-70.

Okunlola, O. A., and Idowu, O., 2012. The geochemistry of claystone-shale deposits from the Maastritchian Patti Formation, Southern Bida Basin, Nigeria. Earth Sciences Research Journal, 16(2), Pp. 57-67.

Omali, A. O., Imasuen, O. I., and Okiotor, M. E., 2011. Sedimentological characteristics of Lokoja Sandstone exposed at Mount Patti, Bida Basin, Nigeria. Advances in Applied Science Research, 2(5), Pp. 317-327.

Ominigbo, O. E., 2022. Evolution of the Nigerian basement complex: Current status and suggestions for future research. Journal of Mining and Geology, 58(1), Pp. 229-236.

Osokpor, J., and Okiti, J., 2013. Sedimentological and paleodepositional studies of outcropping sediments in parts of Southern Middle Niger Basin. International Journal of Science and Technology, 12, Pp. 839-846.

Osokpor, J., Okiti, J., Ekuerugbe, L. O., and Osokpor, O. J., 2013. Paleodepositional environment and sequence stratigraphy of outcropping sediments in parts of Southern Middle Niger Basin, Nigeria. Journal of Environmental and Earth Sciences, 3(9), Pp. 152-170.

Petters, S. W., 1986. Foraminiferal biofacies in the Nigerian rift and continental margin deltas. In M. N. Oti and G. Postma (Eds.), Geology of deltas (pp. 219-235). Balkema.

Pettijohn, F. J., 1984. Sedimentary rocks (3rd ed.). CBS.

Priya, R. K., Tewari, V. C. and Ranjan, R. K., 2021. Geochemical (REE and trace elements) characteristics and tectonic setting discrimination of Permo-Carboniferous sandstone from Sikkim Lesser Himalaya, NE India. Russian Journal of Earth Sciences, 21, ES5002. https://doi.org/10.2205/2021ES000756

Rahaman, M. A. O., Coker, S. J., Bale, R. B., Omada, I. J., Obaje, N. G., and Fadiya, S. L., 2017. Field trip guide to the Southern Bida Basin. NMGS.

Rahaman, M. A. O., Fadiya, S. L., Adekola, S. A., Coker, S. J., Bale, R. B., Olawoki, O. A., Omada, I. J., Obaje, N. G., Akinsape, O. T., Ojo, G. A., and Akande, W. G., 2019. A revised stratigraphy of the Bida Basin, Nigeria. Journal of African Earth Sciences, 151, Pp. 67-81.

Reed, S. R., and Mergner, J. I., 1945. Preparation of rock thin sections (U.S. Geological Survey Report). http://www.mirisocam.org/ammin/am38/am38_1184.pdf

Sanni, Z. J., Toyin, A., Ibrahim, A., and Ayinla, H. A., 2016. Provenance studies through petrography and heavy mineral analysis of part of Agbaja-Lokoja Formation, Bida Basin, NW Nigeria. Ife Journal of Science, 18(1), Pp. 203-212.

Suttner, L. J., Basu, A., and Mach, G. H., 1981. Climate and the origin of quartz arenites. Journal of Sedimentary Petrology, 51, Pp. 1235-1246.

Wright, J. B., Hastings, D. A., Jones, W. B., and Williams, H. R., 1985. Geology and mineral resources of West Africa. George Allen and Unwin.

Zaborski, P. M., 1998. A review of the Cretaceous system in Nigeria. African Geosciences Review, 5, Pp. 385-483.